12

Clay Minerals (1995) **30**, 239–248

REE DISTRIBUTION IN PRESENT-DAY AND ANCIENT SURFACE ENVIRONMENTS OF BASALTIC ROCKS (CENTRAL PORTUGAL)

M. I. PRUDÊNCIO, M. A. GOUVEIA AND M. A. SEQUEIRA BRAGA*

*Departamento de Química, ITN, Estrada Nacional 10, 2685 Sacavém, Portugal, and * Universidade do Minho, Ciências da Terra, 4719 Braga codex, Portugal*

(*Received 1 July 1994; revised 27 March 1995*)

ABSTRACT: Rare earth elements are mobilized, fractionated and precipitated during weathering processes of basaltic rocks of the Lisbon Volcanic Complex. In general there is an increase in the *REE* contents in the whole samples with increasing weathering and fractionation between *LREE* and *HREE*. Cerium is partially oxidized and Ce^{4+} is retained resulting in negative Ce anomalies in the whole samples of the base and middle profile zones. In the clay fraction there is an increase in the *REE* contents from the top to the bottom of the profiles, except for Ce, giving rise to positive Ce anomalies in the top and negative anomalies of this element in the middle and bottom of the profiles. Significant positive Ce anomalies occur in the finer fractions of palaeoweathered (Upper Cretaceous/ Lower Eocene) basalts associated with low *REE* contents relative to the whole samples indicating more intense leaching conditions in the Upper Cretaceous/Lower Eocene than at the present day. However, in both cases no positive Ce anomalies were found in the whole samples. There appears to be a negative correlation between the $(La/Yb)_{ch}$ ratio variation and the clay mineralogy/drainage conditions.

The rare earth elements' (*REE*) behaviour in surface weathering environments has been the subject of numerous works especially in the last two decades, contributing to our understanding of how these elements behave under different conditions of weathering. However, the results obtained so far are sometimes varied and a large number of studies was undertaken to confirm the use of *REE* for the original parent rock, based only on the *REE* patterns of the whole samples (fresh rock up to the soil). There are four main types of *REE* behaviour: (1) *REE* are immobile (Bonnot-Courtoix, 1981; Kholodov, 1972); (2) *REE* are slightly mobilized (Steinberg & Courtois, 1976); (3) *REE* are mobilized without fractionation (Burkov & Podporina, 1970; Kronberg *et al.*, 1987; Melfi *et al.*, 1990; Decarreau *et al.*, 1979) and (4) *REE* are mobilized and fractionated during weathering (Bliskovskiy *et al.*, 1969; Nesbitt, 1979; Duddy, 1980; Schieber, 1988; Topp *et al.*, 1985; Fortin, 1989; Bonnot-Courtoix & Flicoteaux, 1989; Banfield & Eggleton, 1989; Braun *et al.*, 1990).

As far as the *REE* behaviour during weathering of basaltic rocks in a continental environment is concerned, only a small number of studies have been carried out. Results obtained by Melfi *et al.*, 1990 and by Malengreau (1990) from Paraná basalts (Brazil) showed that Ce is concentrated in the surficial level and the trivalent *REE* may be strongly mobilized without fractionation, suggesting that these elements are removed mechanically and incorporated in the secondary phases (clay minerals and oxides).

The Lisbon Volcanic Complex (LVC), from the Upper Cretaceous/Lower Eocene, is an alkali basalt/ basanitic suite, formed by intra-continental rifting. The LVC has been intensely weathered and eroded. Palaeosoils and sedimentary deposits occur intercalated with lava flows and tuffs, indicating large intervals of time between magmatic episodes (Serralheiro, 1978). The Cretaceous climate was hot and moist (Furon, 1950; Parrish, 1982; Tardy, 1986). In the Tertiary a cooling process began, and a tropical climate gave rise to a temperate climate at the beginning of the Quaternary. The prevailing climate is temperate (500–800 mm annual rainfall; 3–5 dry months; mean annual temperature = 16.9°C). The present-day soils are, in general, <50 cm thick.

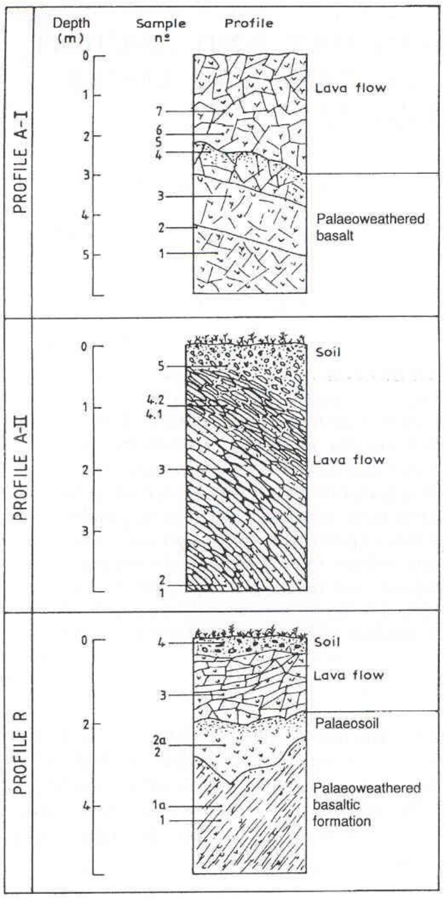

FIG. 1. The weathering profiles at Alfragide (A-I and A-II) and Restelo (R).

Studies of the *REE* distribution during weathering of basalts from central Portugal (LVC included) have shown that, under the prevailing temperate climate, these elements are released from the primary minerals and mobilized downwards by meteoric waters (Prudêncio *et al.*, 1990, 1993; Prudêncio, 1993). Cerium is partially oxidized and retained (co-precipitates with Fe oxides in the presence of Mn and P), while trivalent *REE* are mobilized, causing Ce anomalies. Under favourable conditions, these elements may be precipitated. Neodymium and the middle *REE* are concentrated in phosphates (Prudêncio *et al.*, 1993), and enrichments of the middle *REE* in apatite have already been observed during early diagenesis (Schmitz *et al.*, 1988; Elliot, 1993). Isovolume balance calculations in LVC weathering profiles showed that in general there are losses of *REE* in the top and gains in the middle and base of the profiles. The heavy *REE* (*HREE*) are in general more mobilized than the light *REE* (*LREE*): (1) losses in the top – up to 35% for La and up to 40% for Lu; and (2) gains in the base – up to 40% for La and up to 90% for Lu (Prudêncio, 1993).

Previous studies showed that dioctahedral smectites (Fe- and Mg-rich) are the dominant clay minerals present in the clay fractions (<2 μm) formed by weathering of basalts from central Portugal. Kaolinites (halloysites), micas and palygorskite are also present. Interstratified minerals are rare. The clay mineralogy depends mainly on the drainage conditions, and in general halloysites occur in higher land, whilst smectites dominate in lower land (Prudêncio, 1993). In this work the *REE* distribution in palaeoweathered basalts of the LVC was studied and compared with present-day or recently weathered basaltic rocks, in order to evaluate the use of these elements as fingerprints of palaeoclimates. Three selected profiles are described, including basalts with different structures and ancient and present-day weathering levels. The clay minerals and the *REE* distribution in the whole samples and the respective clay fractions of weathered basalts and soils, as well as in different size-fractions of present-day and ancient surface levels, were studied.

EXPERIMENTAL

Samples and methods

Whole samples collected at different levels of three weathering profiles and the respective clay fractions were studied. For the ancient and present-day surficial levels, the following size fractions were also analysed — <2 μm, 2 μm–20 μm, 20 μm–63 μm, 63 μm–2 mm, and ⩾ 2mm. The clay fractions were separated by successive centrifugations. The other fractions were obtained by sedimentation and sieving techniques. No chemical treatments were employed.

Mineralogical analyses were made by X-ray diffraction (Cu-K_α radiation). Mineral percentages of clay minerals in the clay fractions were obtained using oriented aggregates, by measuring relative intensity peaks (001). The clay fraction present in palaeoweathered levels is <2% and in the present-day surface levels is 5%.

The *REE* contents were obtained by using instrumental neutron activation analysis (INAA) method. Irradiations were made on the Portuguese Research Reactor, with a neutron flux of 3.2 × 10^{12} n cm^{-2} s^{-1} (Prudêncio *et al.*, 1986; Gouveia *et al.*, 1992). Basalt GSR-3 and andesite GSR-2 of the Institute of Geophysical and Geochemical Exploration from the People's Republic of China were used as standards.

Weathering profiles: petrographic and mineralogical features, sampling

The weathering profiles are located near Lisbon, two in Alfragide (A) and one in Restelo (R), and are schematically represented in Fig. 1.

Alfragide: profiles A-I and A-II. These are similar topographic conditions, near the top of a small hill, and ~100 m apart). Profile A-I is a palaeoweathered lava flow overlain by a massive lava flow. (1) The palaeoweathered zone (samples 1–4) consists of a skeletal framework of pyroxenes, large amphibole phenocrysts and olivine grain relics in a clay-ferruginous plasma. Sample 4 refers to an ancient surface level, still preserving the initial texture with evidence of metamorphism caused by the subsequent lava flow (Prudêncio, 1993). (2) The overlying lava flow has a porphyritic texture — olivine and clinopyroxene phenocrysts are set in a groundmass with a microgranular texture, comprising plagioclase, clinopyroxene, olivine, biotite, glass and Fe-Ti oxides. Samples 5–7 refer to weathered basalt collected at different depths.

The clay minerals are 90–95% smectites and 5–10% halloysites (7.3 Å) in the palaeoweathered zone. In the overlying lava, smectites decrease upwards (85%–60%), halloysite increases (15%–30%), and palygorskite occurs only in the upper sample analysed (10%).

Profile A-II is a lava flow showing spheroidal weathering with an abrupt change between the fresh black basalt and the weathered rock giving rise to a well-drained profile. The basalt has an intergranular texture in which olivine, clinopyroxene and ulvospinel grains are surrounded by large feldspars laths. Samples were collected at different depths, corresponding to different weathering degrees from the base (sample 1) up to the soil (sample 5). Samples 4.1 and 4.2 correspond to a relatively fresh basalt and the adjacent weathered material, respectively.

The clay minerals are 80–90% halloysite (7.3 Å), <20% micas and <10% palygorskite, with an increase in the halloysite and palygorskite contents up through the profile, associated with a decrease in the mica content. No smectites were found in the clay fractions of this weathered basalt, which is rare in the LVC complex, and this is due to the very good drainage conditions (Prudêncio, 1993).

Restelo: profile R (top of a small hill). Profile R includes an intensely palaeoweathered reddish basaltic formation, which presents a very homogeneous meteoric calcitization (Prudêncio *et al.*, 1994). Samples 1 and 1a refer to calcitized and non-calcitized weathered basaltic samples, respectively. At the top of this formation there is a palaeosoil, where calcite has been dissolved (samples 2 and 2a). Overlying this formation there is a lava flow (sample 3) with a present-day soil ~20 cm thick (sample 4).

The palaeoweathered formation has an intergranular texture — olivine and pyroxene phenocrysts are surrounded by feldspars, pyroxenes and Fe-Ti oxides. There are large vacuoles filled by calcite. The overlaid lava flow presents an intergranular texture, with large phenocrysts of olivine and clinopyroxene in an intergranular matrix composed of feldspars, pyroxenes and oxides. The clay mineralogy is dominated by smectites in all levels of the profile, with only trace amounts of halloysite, micas and palygorskite.

RARE EARTH ELEMENT DISTRIBUTION

The *REE* data measured for the whole samples and different size-fractions are given in Tables 1 and 2, together with Σ*REE*, $(La/Yb)_{ch}$ and Ce/Ce*. The chondrite data used for normalizing the *REE* contents are also listed in Table 1 (Haskin *et al.*, 1971).

Profile A-I

(a) Palaeoweathered zone. The *REE* patterns of the whole samples analysed (1–4) are similar, with a slight negative Ce anomaly (Table 1, Fig. 2).

The *REE* patterns of the clay fractions clearly show a positive Ce anomaly, especially samples 3 and 4 (Ce/Ce* = 1.44 and 1.42, respectively,

TABLE 1. *REE* data of the whole samples from profiles A-I, A-II and R.

Profile	Sample	La	Ce	Nd	Sm	Eu	Tb	Yb	Lu	Σ*REE*	$(La/Yb)_{ch}$	Ce/Ce^*
		Concentration (ppm)										
A-I	7	59	116	60	11.6	3.48	1.8	2.0	0.31	254	17.5	0.87
	6	51	102	54	9.50	2.92	1.4	1.5	0.22	223	20.9	0.87
	5	53	103	57	10.7	3.26	1.4	1.5	0.21	230	21.6	0.85
	4	84	146	82	14.5	4.24	1.9	2.5	0.40	336	20.3	0.77
	3	63	125	74	12.4	3.35	1.9	2.0	0.22	282	19.0	0.84
	2	58	123	65	11.1	3.15	1.9	1.6	0.22	264	21.8	0.92
	1	79	159	80	14.1	4.13	1.9	2.6	0.37	341	18.2	0.89
A-II	5	90	183	117	22.9	6.88	3.5	4.1	0.57	428	13.3	0.84
	4.2	93	157	120	23.6	7.10	3.1	4.1	0.56	409	13.8	0.70
	4.1	64	102	59	10.5	3.22	1.4	2.0	0.26	242	19.4	0.72
	3	72	154	106	21.4	6.37	3.4	3.4	0.53	367	12.8	0.86
	2	82	172	109	20.5	6.18	3.1	4.1	0.54	397	12.1	0.86
	1	59	105	62	10.9	3.37	1.8	2.2	0.34	245	16.3	0.77
R	4	55	112	61	11.0	3.20	1.5	2.0	0.38	246	16.7	0.87
	3	53	105	58	10.6	3.04	1.4	2.1	0.30	233	15.3	0.85
	2a	57	111	62	11.1	3.25	1.4	2.1	0.33	249	16.5	0.84
	2	51	97.7	53	9.74	2.86	1.2	1.8	0.27	218	17.2	0.74
	1a	50	99.0	54	9.90	2.93	1.3	1.9	0.32	219	16.0	0.86
	1	36	69.7	38	6.90	2.01	0.76	1.4	0.24	155	15.6	0.84
Chondrites (Haskin *et al.*, 1971)		0.33	0.88	0.6	0.181	0.069	0.047	0.2	0.034			

$La/Yb_{ch} = (La/La_{ch})/(Yb/Yb_{ch})$; $Ce/Ce^* = 3Ce/Ce_{ch}/(2La/La_{ch}) + (Nd/Nd_{ch})$

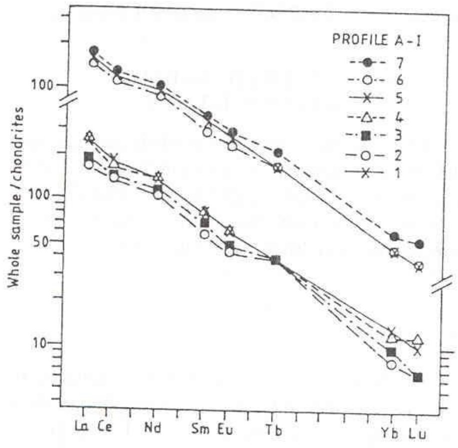

FIG. 2. Chondrite-normalized patterns for the whole samples of profile A-I (Alfragide).

Table 2). The anomaly is more evident when this fraction is compared with the whole samples (Fig. 3). The *REE* contents are, in general, lower in the clay fractions than in the whole samples. They increase upwards until sample 3 and decrease significantly in the palaeosoil — sample 4 (Table 2). Thus, the clay fraction of the upper level of the palaeoweathered zone has the lower values of the *REE* contents and a significant positive Ce anomaly (Fig. 3).

The *REE* patterns of the ancient surface level (sample 4) show a decrease in the *REE* contents with decreasing grain size, except for Ce, causing a negative anomaly of this element in the coarser fractions and a positive anomaly in the finer fractions (Fig. 4, Table 2).

(b) Lava flow with present-day surface level. The *REE* patterns for the whole sample show a slight negative Ce anomaly and the upper sample has the higher *REE* contents (samples 5–7, Table 1, Fig. 2).

TABLE 2. *REE* data of different size-fractions of samples from profiles A-I, A-II and R.

Profile	Sample	Size fraction (μm)	Concentration (ppm)										
			La	Ce	Nd	Sm	Eu	Tb	Yb	Lu	*REE*	$(La/Yb)_{ch}$	Ce/Ce^*
A-I	7	<2	76	182	103	17.9	5.39	2.4	3.5	n.a.	>390	13.1	0.98
	6	<2	181	251	296	51.9	14.4	4.6	4.3	n.a.	>803	25.6	0.54
	4	<2	36	118	39	6.58	2.02	0.94	1.2	0.16	204	18.2	1.42
	3	<2	45	151	52	8.96	2.59	1.2	1.5	0.20	263	18.2	1.44
	2	<2	46	113	48	8.49	2.48	1.1	1.7	0.20	221	16.4	1.07
	1	<2	55	140	57	9.82	2.82	1.3	2.1	0.35	268	15.6	1.11
A-II	5	<2	124	264	132	22.0	6.65	2.8	4.1	0.46	556	18.4	0.93
	3	<2	170	353	249	44.5	12.7	5.0	6.6	0.93	842	15.7	0.83
	2	<2	195	305	288	50.5	14.4	5.3	6.8	0.65	866	17.4	0.63
	1	<2	222	357	305	53.0	15.3	5.9	7.3	0.90	966	18.4	0.66
A-I	4	<2	36	118	39	6.58	2.02	0.94	1.2	0.16	204	18.2	1.42
		2–20	60	163	66	11.4	3.37	1.1	2.0	0.32	307	18.2	1.17
		20–63	58	141	61	10.9	3.27	1.1	2.0	0.40	278	19.6	1.06
		63–2 mm	70	142	70	12.3	3.74	1.5	2.5	0.34	302	17.0	0.89
		>2 mm	91	151	89	15.3	4.65	2.0	2.6	0.39	356	21.2	0.74
R	4	<2	30	67.2	28	4.84	1.34	0.69	1.1	0.19	133	16.5	1.00
		2–20	79	156	76	12.7	3.75	1.6	2.4	0.35	332	19.9	0.88
		20–63	36	80.6	51	9.9	3.02	1.4	1.6	0.30	184	13.6	0.91
		63–2 mm	52	102	57	10.4	3.11	1.5	2.0	0.33	228	15.8	0.85
		>2 mm	58	115	61	11.2	3.35	1.5	2.1	0.35	253	16.8	0.87
R	2a	<2	15	122	12	2.10	0.57	n.a.	0.39	0.11	>152	14.1	3.79
		2–20	16	154	14	2.43	0.67	0.27	0.44	n.a.	>188	21.8	4.41
		20-63	8.8	59	10	1.77	0.51	n.a.	0.39	n.d.	>81	13.8	2.83
		63–2 mm	24	52.7	27	4.98	1.45	0.78	0.82	0.16	112	17.8	0.94
		>2 mm	64	116	71	13.1	3.9	1.5	2.3	0.40	272	16.9	0.78

n.a. — not analysed; n.d. — not detected; $(La/Yb)_{ch} = (La/La_{ch})/(Yb/Yb_{ch})$;
$Ce/Ce^* = 3Ce/Ce_{ch}/(2La/La_{ch}) + (Nd/Nd_{ch})$

There is a negative Ce anomaly in the deeper clay fraction sample and Nd appears to be the most enriched *REE* when compared with the whole samples (Fig. 3).

Profile A-II

There is an increase in the *REE* contents in the whole samples, especially Nd, with weathering and a negative Ce anomaly at all levels of the profile (Table 1, Fig. 5).

There is a negative Ce anomaly especially in the deeper clay fraction samples associated with high total *REE*s (Table 2, Fig. 6). The *REE* contents decrease up through the profile, even when compared with the respective whole samples. Cerium tends to remain in the top, causing positive Ce anomalies in this level relative to the whole sample from the same level and negative Ce anomalies in deeper zones. The *REE* are concentrated in the clay fraction relative to the whole samples.

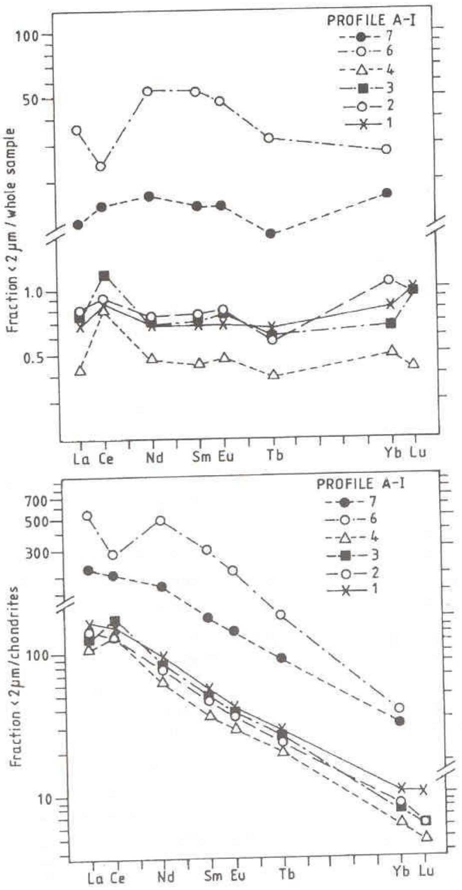

FIG. 3. *REE* distributions of the clay fractions from profile A-I relative to chondrites and to the corresponding whole samples.

Profile R

The *REE* patterns for whole samples are similar to each other, with a slight negative Ce anomaly (Fig. 7). Sample 1 (calcitized basalt) has the lowest values for all of the *REE*, and this is certainly due to calcite dilution (Table 1).

The *REE* patterns of the size-fractions of the palaeosoil (sample 2a) and the present-day soil (sample 4) (Figs. 8 and 9) mainly show (1) in present-day soil there are no significant anomalies and the clay fraction has the lower *REE* contents (Fig. 8) and (2) in the ancient soil the *REE* contents

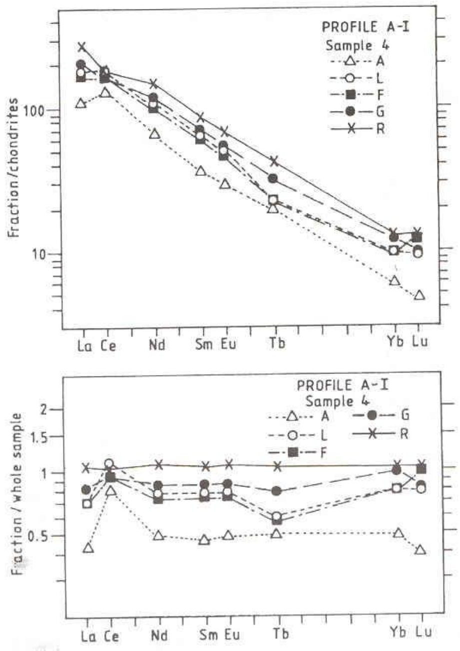

FIG. 4. *REE* distributions of the different size-fractions of sample A-I-4 relative to chondrites and to the whole sample (R: ⩾2 mm, G: 2 mm–63 µm, F: 63 µm–20 µm, L: 20 µm–2 µm and A: <2 µm).

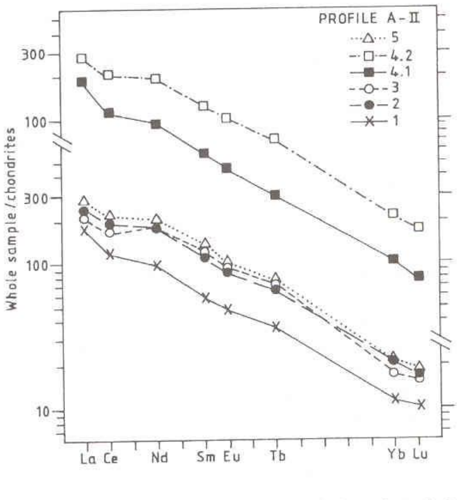

FIG. 5. Chondrite-normalized patterns for the whole samples of profile A-II (Alfragide).

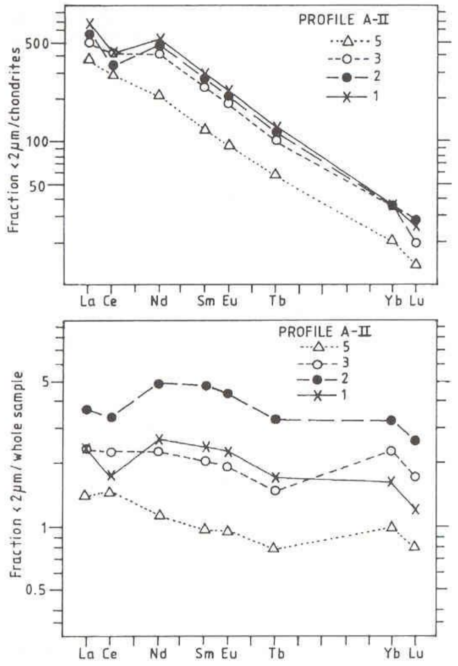

FIG. 6. *REE* distributions of the clay fractions from profile A-II relative to chondrites and to the corresponding whole samples.

of the size-fraction >2 mm are about the same as those found in the whole sample, and most lower values are found in the finer fractions, except for Ce, causing large positive Ce anomalies in these fractions (Table 2). The *REE* contents are more depleted in the palaeoweathered soil relative to the whole samples than in the present-day soil.

DISCUSSION AND CONCLUSIONS

The redistribution of the *REE* during weathering processes and the exact location of these elements in the secondary phases, clay minerals included, are not easy to determine especially if the parent rock, such as basalt, has low concentrations of these elements. Previous work on the *REE* distribution during alteration processes of basalts from the LVC, by using a scanning electron microscope with an energy dispersive system (SEM-EDS), showed the presence of secondary *REE*-rich phosphate phases in a very particular profile with a situation of water saturation during the winter, where a strong enrichment of *REE* in the finer fractions of the weathered basalt occur. The chemical analysis of these phases by EDS showed that Nd always presents the most intense peak and Nd>Ce, in agreement with the general enrichment of Nd, observed in several profiles developed in the LVC. Cerium (Ce^{4+}) was found by SEM-EDS in Fe-rich nodules, but only in the presence of P and Mn (Prudêncio *et al.*, 1993; Prudêncio, 1993). In spite of these, *REE*-rich phosphate phases have been detected only in one particular profile and so it may be concluded that these phases certainly play an important role in the *REE* distribution during weathering processes. However, these elements are also present in other secondary phases and some relations between the *REE* and the clay mineralogy/drainage conditions appear to exist.

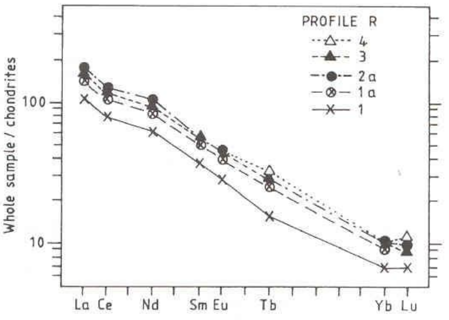

FIG. 7. Chondrite-normalized patterns for the whole samples of profile R (Restelo).

In the three profiles studied, the *REE* concentrations of the whole samples increase up through the basaltic formations (Table 1). However, in the finer fractions, especially the clay fractions, there is a significant decrease in these elements from the base to the top of all basaltic formations, which indicates that *REE* are released by the breakdown of primary minerals and only partially taken up by the secondary phases present in the finer fractions. The other parts of the trivalent *REE* are leached by local meteoric waters from the upper levels of the profiles and concentrated in deeper zones, probably in the form of complexes or by mechanical transport of the secondary phases. Cerium has a different behaviour, being partially oxidized and Ce^{4+} is retained relative to the trivalent *REE*.

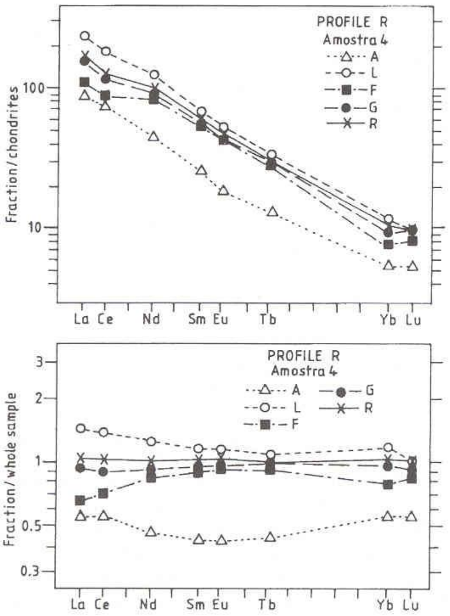

FIG. 8. *REE* distributions of the different size-fractions of sample R-4 relative to chondrites and to the whole sample (R: ⩾2 mm, G: 2 mm–63 μm, F: 63 μm–20 μm, L: 20 μm–2 μm and A: <2 μm).

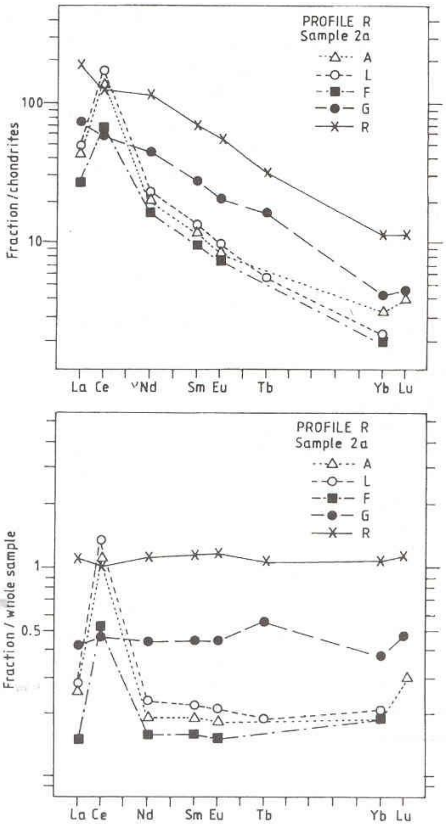

FIG. 9. *REE* distributions of the different size-fractions of sample R-2a relative to chondrites and to the whole sample (R: ⩾2 mm, G: 2 mm–63 μm, F: 63 μm–20 μm, L: 20 μm–2 μm and A: <2 μm).

The strong leaching of the trivalent *REE* associated with a positive Ce anomaly in the clay fractions of palaeoweathered zones compared with the present-day surface levels agree with the idea of a more humid and warmer climate during the Upper Cretaceous/Lower Eocene (Furon, 1950; Parrish, 1982; Tardy, 1986). However, even at that time the climatic conditions seem not to have been intense enough to produce positive Ce anomalies in the whole samples, as has sometimes been found in tropical areas (Braun *et al.*, 1990; Marsh, 1991). The low proportion of *REE* in the finer fractions relative to the whole samples and the positive Ce anomalies observed are thus confirmed as fingerprints for the palaeoweathered formations in the Lisbon Volcanic Complex. Rare earth element distribution can also contribute to further palaeoclimatic studies.

The *REE* distribution analysis in different size-fractions of ancient and present-day surface levels showed that: (1) *REE* contents decrease with decreasing particle size from the size-fraction >2 mm to the size-fraction 20–63 μm, increase in the silt fraction (2–20 μm) and decrease again in the clay fraction. The lower values in the clay fraction compared to the silt fraction may be explained by an easier leaching (and non-uptake of the trivalent *REE* by secondary phases) of the smaller particles. (2) In present-day soil, the Ce/Ce* variation with the particle size is much lower than in the ancient surface levels, where a significant increase in Ce/Ce* with decreasing particle size is found, especially for sample 2a from the Restelo profile (Table 2).

Worthy of note is the decrease in the $(La/Yb)_{ch}$ ratio with increasing weathering and up through the well-drained profile A-II, where halloysites are the dominant clay minerals. In this case the intense leaching conditions may not allow a significant precipitation of *REE* phases and these elements are instead probably retained by clay minerals and/or oxides. The percolating solutions have a higher *HREE/LREE* ratio than the initial basaltic rock and halloysites may more easily accommodate the *HREE* than the *LREE* leading to a general decrease in the proportion *LREE/HREE*.

The LVC has been intensely weathered since its formation and the consequent sedimentary processes may have led to a general addition of *REE* into the weathered complex. Leaching of the *REE* from higher land (halloysite dominant) may occur, associated with an enrichment of these elements in lower land (smectites dominant). However, special attention should be paid to the very low absolute and relative *REE* contents associated with significant positive Ce anomalies in the finer fractions of palaeoweathered basalts and ancient surface levels. These indicate that the trivalent *REE* were strongly leached from these fractions during palaeoweathering, and no significant later addition of these elements in the secondary minerals (clay minerals included) of the finer fractions appears to have occurred.

ACKNOWLEDGMENTS

Thanks are due to JNICT for financial support, and also to the staff of the Reactor Department for their assistance with the neutron irradiations.

REFERENCES

Banfield J.F. & Eggleton R. (1989) Apatite replacement and rare earth mobilization, fractionation and fixation during weathering. *Clays Clay Miner.* **37**, 113–127.

Bliskovskiy V.Z., Mineyev D.A. & Kholodov V.N. (1969) Accessory lanthanides in phosphorites. *Geokhimiya*, **11**, 1348–1361.

Bonnot-Courtois C. (1981) *Géochimie des terres rares dans les principaux milieux de formation et sédimentation des argiles*. PhD thesis, Univ. de Paris-Sud, 217pp.

Bonnot-Courtois C. & Flicoteaux R. (1989) Distribution of rare-earth and some trace elements in Tertiary phosphorites from the Senegal Basin and their weathering products. *Chem. Geol.* **75**, 311–328.

Braun J., Pagel M., Muller J., Bilong P., Michard A. & Guillet B. (1990) Cerium anomalies in lateric profiles. *Geochim. Cosmochim. Acta*, **54**, 781–795.

Burkov V.V. & Podporina E.K. (1970) Some geochemical characteristics of rare (trace) elements in weathering crusts. Translated from *Litoligiya i Poleznye Iskopaemye*, **4**, 55–64.

Decarreau A., Courtois C. & Steinberg M. (1979) Comportement des éléments de la première série de transition et des lanthanides dans les altérations naturelles et expérimentales. *Sci. Géol.* **53**, 29–34.

Duddy I.R. (1980) Redistribution and fractionation of rare-earth and other elements in a weathering profile. *Chem. Geol.* **30**, 363–381.

Elliot W.C. (1993) Origin of the Mg-smectite at the Cretaceous/Tertiary (K/T) boundary at Stevens Klint, Denmark. *Clays Clay Miner.* **41**, 442–452.

Fortin P. (1989) Mobilisation, fractionnement et accumulation des terres rares lors de l'altération latéritique de sédiments argilo-sableux du Bassin de Curitiba (Brésil). PhD thése, Ecole des Mines de Paris, *Mémories des Sciences de la Terre* **10**, 186.

Furon R. (1950) Les problèmes de paléoclimatologie et de paléobiologie posés par la géologie de l'Arctide. *C.R. somm. Séances Soc. Biogéogr.* **230**, 13–23.

Gouveia M.A., Prudêncio M.I., Morgado I. & Cabral J.M.P. (1992) New data on the GSJ reference rocks JB-1a and JG-1a by instrumental neutron activation analysis. *J. Rad. Nuc. Chem.* **158**, 115–120.

Haskin L.A., Helmke P.A., Paster T.P. & Allen R.O. (1971) *Activation Analysis in Geochemistry and Cosmochemistry* (A.O. Brunfelt & E. Steinnes, editors), Universitetsforlaget, Oslo, pp.201–218.

Kholodov V.N. (1972) Behaviour of the rare earths during weathering of the Karatau phosphorites. *Geokhimiya* **9**, 1063–1070.

Kronberg B.I., Tazaki K. & Melfi A.J. (1987) Detailed geochemical studies of the initial stages of weathering of alkaline rocks: Ilha de S.Sebastião, Brazil. *Chem. Geol.* **60**, 79–88.

Malengreau N. (1990) Comportement des terres rares et évolutions des compositions isotopiques du Sr et du Nd dans un perfil d'altération développé sur roches basiques. *Repport du DEA Géosciences de l'Énvironment, Université d'Aix-Marseille III.*

Marsh J.S. (1991) *REE* fractionation and Ce anomalies in weathered Karoo dolerite. *Chem. Geol.* **90**, 184–194.

Melfi A.J., Figueiredo A.M., Kronberg B.I., Dohert W.D. & Marques L.S. (1990) *REE* mobilities during incipient weathering of volcanic rocks of the Paraná basin, Brazil. *Chem. Geol.* **84**, 375–376.

Nesbitt H.W. (1979) Mobility and fractionation of rare earth elements during weathering of a granodiorite. *Nature* **279**, 206–210.

Parrish B. (1982) Causes and consequences of the relation between area and age of the ocean floor. *J. Geophys. Res.* **87**, 289–302.

Prudêncio M.I. (1993) *Geoquímica de superfície em rochas basálticas continentais (Portugal). Comportamento das terras raras.* Tese de doutoramento, Univ. Minho, Portugal.

Prudêncio M.I., Gouveia M.A. & Cabral J.M.P. (1986) Instrumental neutron activation analysis of two French geochemical reference samples — basalt BR and biotite Mica-Fe. *Geostand. Newsl.* **X**, 29–31.

Prudêncio M.I., Sequeira Braga M.A.S. & Cabral J.M.P. (1990) Geoquímica de superfície das terras raras em rochas basálticas do Complexo Vulcânico de Lisboa. *VIII Semana de Geoquímica, Lisboa, Portugal.*

Prudêncio M.I., Sequeira Braga M.A.S. & Gouveia M.A. (1993) *REE* mobilization, fractionation and precipitation during weathering of basalts. *Chem. Geol.* **107**, 251–254.

Prudêncio M.I., Gouveia M.A., Sequeira Braga M.A.S. & Figueiredo M.O. (1994). *REE* distribution as an indicator of the origin of carbonates and silicates in basaltic rocks. VM Goldschimdt Conference, Edinburgh, 1994, *Mineral. Mag.* **58A**, 744–745.

Schieber J. (1988) Redistribution of rare earth elements during diagenesis of carbonate rocks from the mid-Proterozoic Newland Formation. *Chem. Geol.* **69**, 111–126.

Schmitz B., Anderson P. & Dahl J. (1988) Iridium, sulfur isotopes and rare earth elements in the Cretaceous/Tertiary boundary clay at Stevens Klint, Denmark. *Geochim. Cosmochim. Acta* **52**, 229–236.

Steinberg M. & Courtois C. (1976) Le comportement des terres rares au cours de l'altération et ses conséquences. *Bull. Soc. Géol. France* **1**, 13–20.

Serralheiro A. (1978) *Contribuição para a actualização do conhecimento do complexo vulcânico de Lisboa.* Univ. Lisboa, Portugal.

Tardy Y. (1986) *Le cycle de l'eau. Climats, paléoclimats et géochimie global.* Masson, 338 pp.

Topp S.E., Salbu B., Roaldset E. & Jørgensen P. (1985) Vertical distribution of trace elements in laterite soil (Suriname). *Chem. Geol.* **47**, 159–174.